

Chapter 3. Gas Source Molecular Beam Epitaxy of Compound Semiconductors

Academic and Research Staff

Professor Leslie A. Kolodziejski, Dr. Gale S. Petrich

Visiting Scientists and Research Affiliates

Dr. Hisashi Kanie¹

Graduate Students

Joseph F. Ahadian, Jay N. Damask, Sean M. Donovan, Philip A. Fisher, Easen Ho, Jody L. House, Kuo-Yi Lim, Elisabeth A. Marley, Kan Lu, Xiaofeng Tang

Undergraduate Students

James R. Geraci

Technical and Support Staff

Charmaine A. Cudjoe-Flanders, Angela R. Odoardi

3.1 Introduction

This research program utilizes the chemical beam epitaxy laboratory and emphasizes the epitaxial growth of a wide variety of compound semiconductors (both II-VI and III-V), as well as multilayered structures composed of II-VI/II-VI, II-VI/III-V and III-V/III-V heterostructures. The chemical beam epitaxy laboratory consists of two gaseous source epitaxy reactors (II-VI dedicated and III-V dedicated) interconnected to several smaller chambers which are used for sample introduction and *in-situ* surface analysis and metalization. Such a multi-chamber epitaxy system allows the fabrication of the aforementioned heterostructures within a continuous ultrahigh vacuum environment. The interconnected reactors enable an additional degree of freedom in device design by providing the ability to integrate the II-VI and III-V material families into a single device. For example, a variety of structures are grown (1) in a single reactor for binary or alloy II-VI or III-V epilayers, (2) with both reactors as in the case of II-VI/III-V heterostructures and quantum wells, and (3) in a single reactor as in the case of superlattice structures.

The III-V gas source molecular beam epitaxy (GSMBE) reactor uses solid elemental sources of Ga, In, Al, Si and Be and gaseous hydride sources of arsenic and phosphorus. The II-VI reactor cur-

rently uses solid elemental sources of Zn and Se and gaseous hydrogen selenide, in addition to a nitrogen plasma source and a solid ZnCl₂ source, to achieve p- and n-type doping, respectively. The plasma source is also used with a high purity hydrogen/argon mixture for hydrogen plasma cleaning of GaAs and ZnSe substrates. The highlighted region in figure 1 illustrates the wide range of lattice parameters and energy bandgaps which are accessible using the modular interconnected epitaxy system for the growth of II-VI and III-V compound semiconductors.

In the next section, we will describe our progress in the growth and doping of ZnSe using gas source molecular beam epitaxy; the II-VI effort is complemented by an investigation of the growth of ZnSe on alternative epitaxial III-V buffer layers. An additional II-VI/III-V effort involves the fabrication of ZnSe/GaAs quantum well structures, focusing on the formation of and resultant properties of the ZnSe/III-V heterovalent interface. The III-V GSMBE system is also utilized for the fabrication of (In,Ga)(As,P) waveguide devices that operate as filters at 1.55 μm , which is the wavelength used for optical fiber communication. Additional III-V-based projects include the fabrication of optoelectronic devices on premetalized GaAs MESFET integrated circuits for optoelectronic integrated circuits, an investigation into the growth of GaAs on patterned

¹ Professor, Science University of Tokyo, Japan.

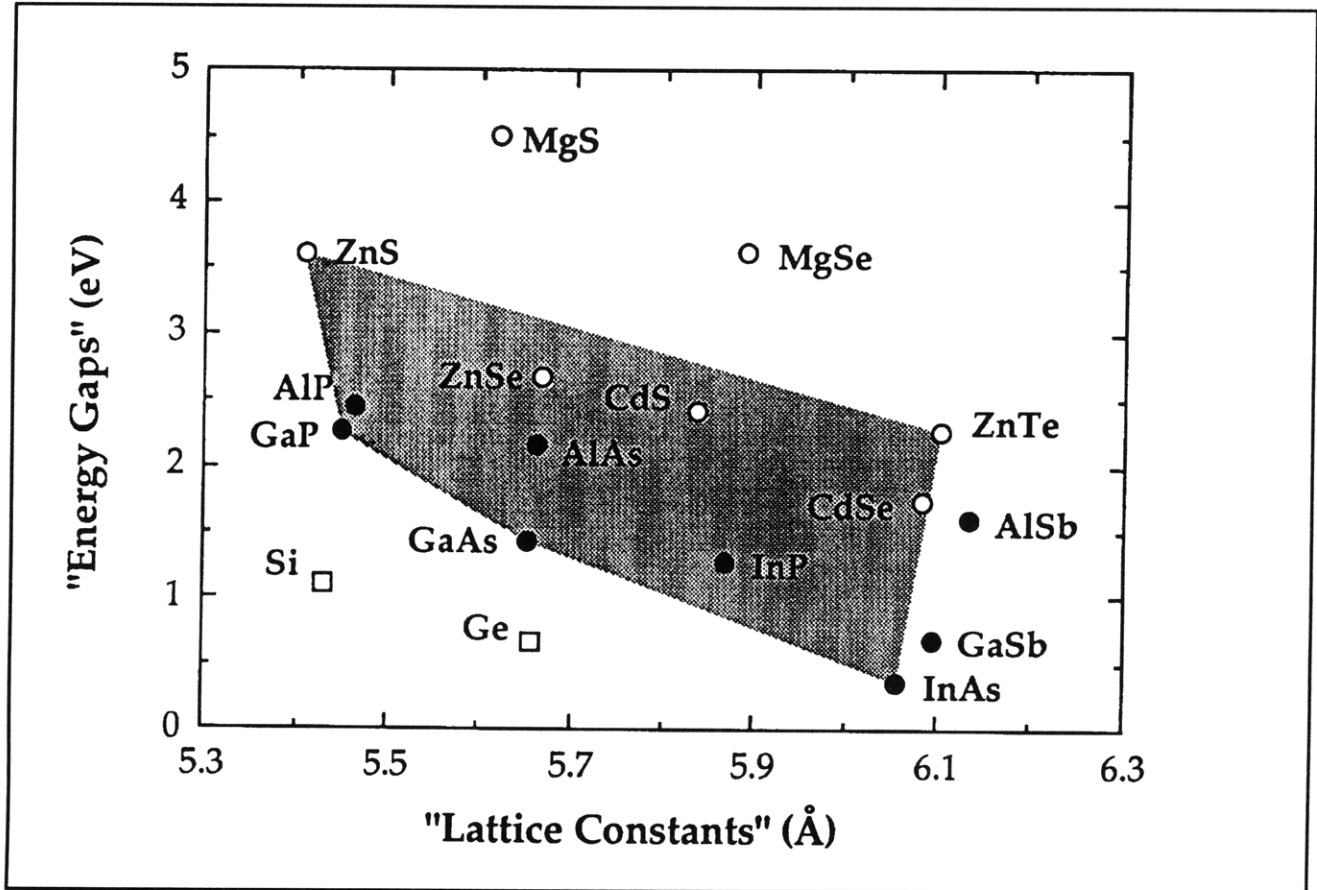


Figure 1. Energy bandgap as a function of lattice parameter for a wide variety of technologically important II-VI and III-V compound semiconductors. The highlighted region indicates the materials, heterostructure combinations, and quantum well structures which are accessible for study utilizing the modular interconnected epitaxy system.

Si substrates, and the fabrication of air bridge microcavities using the concepts of photonic bandgap crystals.

Project Staff

Professor Leslie A. Kolodziejski, Dr. Gale S. Petrich, Philip A. Fisher, Easen Ho, Jody L. House, James R. Geraci

3.2 Gas Source Molecular Beam Epitaxy of ZnSe, ZnSe:Cl and ZnSe:N

Sponsors

- Advanced Research Projects Agency
Subcontract 284-25041
- Joint Services Electronics Program
Contract DAAL03-92-C-0001
Grant DAAH-04-95-1-0038
- National Center for Integrated Photonic Technology
Contract 542-381
Grant subcontract 652-693
- U.S. Army Research Office/ AASERT
Contract DAAH04-93-G-0175

Under the university research initiative (URI) program sponsored by the Advanced Research Projects Agency through the Office of Naval Research, Professor Kolodziejski is a co-principal investigator along with Professor R.L. Gunshor, Purdue University, and Professor A.V. Nurmikko, Brown University. The focus of the URI is aimed towards achieving continuously operating, room temperature, short wavelength, visible light emitters operating in the blue and blue/green spectral ranges based on wide bandgap II-VI semiconductors. As the research effort continues toward eliminating the various technological barriers prohibiting the achievement of viable, commercial "blue" laser diodes, the heterostructures are becoming increasingly complex, requiring the use of advanced epitaxial growth techniques. Gas source molecular beam epitaxy (GSMBE) and/or chemical beam epitaxy (CBE) are anticipated to offer key advan-

tages for growing sophisticated heterostructures containing alloys composed of high vapor pressure species such as S and Se. The use of precision mass flow controllers, which provide a constant, uniform flux of gaseous species, eliminates the need for thermal effusion ovens operating at very low temperatures. The GSMBE technique will be particularly useful for the growth of both ternary and quaternary layers where two high vapor pressure group VI species are required, such as for Zn(Se,Te) or (Zn,Mg)(Se,S). In this project, the growth of ZnSe by GSMBE is being explored with particular emphasis on the controlled incorporation of donor and acceptor species for eventual fabrication of optical devices.

Using sources of elemental Zn and gaseous H₂Se, that was typically thermally decomposed at 1000°C, the ZnSe epilayers were doped p-type with atomic nitrogen derived from a radio frequency plasma source and n-type with chlorine from a ZnCl₂ effusion cell to film thicknesses of 1.5 to 4 μm. The substrate temperature was monitored using an optical pyrometer that was calibrated to the eutectic phase transition of 500 Å of Au on Ge. For the n-type layers, the substrate temperature during growth was 290°C; while for the p-type layers, the substrate temperature ranged from 250°C to 370°C. The Zn deposition rate was measured by depositing Zn onto a water-cooled crystal oscillator located at the substrate position. The H₂Se gas flow was adjusted to maintain a Zn-to-Se surface stoichiometry near unity. The surface stoichiometry was monitored by observing the reflection high energy electron diffraction surface reconstruction. For the p-type films, the nitrogen flow was regulated by a leak valve resulting in chamber pressures that ranged from 5.8 × 10⁻⁷ to 2.1 × 10⁻⁵ Torr. For the n-type films, the amount of chlorine incident onto the surface was controlled by the ZnCl₂ effusion cell temperature.

The optical properties of the epitaxial ZnSe layers were measured using low temperature photoluminescence (PL). The PL spectra were measured by optically exciting the samples with the 3250 Å line of a focused He-Cd laser, providing a power density of approximately 300 mW/cm². The luminescence was analyzed with a 0.5 m spectrometer and a photomultiplier. The PL spectra from the undoped ZnSe layers were dominated by the donor-bound exciton (I₂) and free exciton (E_x) transitions. The Y₀ and I_v transitions which have been reported to be observed in undoped ZnSe films were also

detected. Shahzad et. al.² have reported ZnSe films with carrier concentrations of ~ 10¹⁵ cm⁻³ grown on GaAs substrates exhibiting similar PL features. Hall effect measurements of the undoped GSMBE-grown layers showed n-type conductivity with carrier concentrations ranging from high 10¹⁵ cm⁻³ to low 10¹⁷ cm⁻³.

Chlorine-doped ZnSe samples were analyzed using secondary ion mass spectroscopy (SIMS), photoluminescence, capacitance-voltage (C-V) measurements, and Hall effect measurements. The chlorine concentration, which varied from 9 × 10¹⁵ cm⁻³ to 8 × 10¹⁹ cm⁻³, was primarily measured with SIMS. For doping concentrations greater than 10²⁰ cm⁻³, the growth rate decreased to below 1000 Å/hr, even though the undoped ZnSe growth rate was ~ 7000 Å/hr for identical growth conditions. The decrease in the growth rate is speculated to be due to a surface chemical reaction involving the Cl and the H present at the growth front in the GSMBE environment. The PL spectra of the ZnSe:Cl films with Cl concentrations up to 4 × 10¹⁸ cm⁻³ were dominated by a donor-bound excitonic transition at 2.795 eV with negligible defect-related deep level emission. At a Cl concentration of 8 × 10¹⁹ cm⁻³, the PL spectrum was dominated by a broad band of deep level emission centered at 2.2 eV.

Since thermally decomposed H₂Se is used as a source gas, the presence of hydrogen within the ZnSe lattice was investigated. SIMS was used to measure the amount of hydrogen that was incorporated during the chlorine doping of ZnSe epilayers. As seen in figure 2, the hydrogen concentration remains at or near the background level even though the Cl concentration was varied from < 10¹⁷ cm⁻³ to 3 × 10¹⁸ cm⁻³, suggesting that Cl and H do not form a H-Cl complex. Electrical measurements of the epilayers indicated that the free electron concentration was comparable to the amount of Cl incorporated and that the electrical activation of the Cl donors was negligibly affected by the presence of hydrogen.

Nitrogen-doped ZnSe epilayers were primarily characterized by photoluminescence, secondary ion mass spectroscopy, and capacitance-voltage measurements. Low temperature photoluminescence showed that as the nitrogen concentration increased, the spectra evolved from one exhibiting a neutral N acceptor peak at 2.793 eV to spectra exhibiting a dominant donor-to-acceptor pair (DAP) transition with easily resolved longitudinal optical

² K. Shahzad, J. Petruzzello, D.J. Olego, D.A. Cammack, and J.M. Gaines, "Correlation Between Radiative Transitions and Structural Defects in Zinc Selenide Epitaxial Layers," *Appl. Phys. Lett.* 57: 2452-2455 (1990).

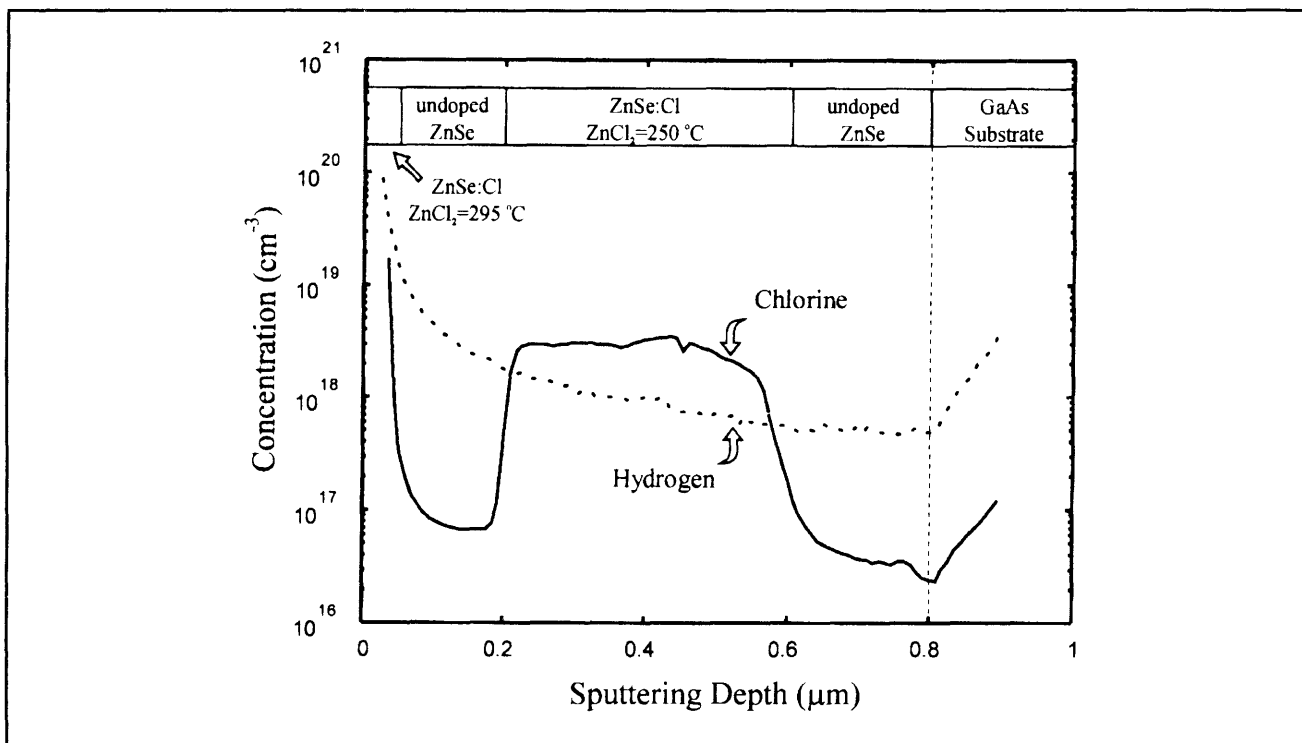


Figure 2. SIMS profile of a ZnSe:Cl structure grown by GSMBE with various ZnCl_2 effusion cell temperatures, as indicated schematically at the top of the figure. The high level of [H] near the surface is an artifact due to surface contamination.

phonon replicas, and finally to spectra exhibiting a single broad DAP feature. Using SIMS, the ZnSe:N epilayers that were grown with a Zn-rich surface stoichiometry, were found to exhibit measurable quantities of nitrogen atoms, while ZnSe:N epilayers that were grown with a Se-rich surface stoichiometry, were found to have N concentrations at or below the SIMS detection level (approximately 10^{17} cm^{-3}). The highest N concentration obtained thus far using GSMBE was $6 \times 10^{18} \text{ cm}^{-3}$. However, C-V measurements indicated that the ZnSe:N films were insulating instead of conductive.

The inability to achieve p-type conductivity suggested that the presence of hydrogen and its electrical passivation of the acceptors may be playing a role. Therefore, to examine the hydrogenation behavior of ZnSe:N films grown by GSMBE and MBE, an in-depth investigation using SIMS was initiated. In the case of GSMBE, the hydrogen was supplied by the thermal decomposition of H_2Se . Figure 3 shows a SIMS profile of a ZnSe:N layer that was grown by GSMBE on a p-type GaAs

substrate. An initial undoped layer of ZnSe was grown to provide a reference for the detection limits of the nitrogen and hydrogen concentrations ([N] and [H] respectively). Two other thin undoped layers were also grown in an otherwise uniformly doped ZnSe:N layer. As the figure shows, the [H] tracks the variation in the [N] throughout the film, decreasing to their respective background levels in the undoped layers. A similar hydrogenation behavior has been observed in other films that were grown under various Zn-to-Se ratios and doping conditions in which the [N] ranged from $\sim 10^{17} \text{ cm}^{-3}$ to $\sim 10^{19} \text{ cm}^{-3}$. The [H] relative to the [N] and their synergistic behavior suggest that N-H bonds may be formed within the lattice, leading to the observed electrical passivation. This is in agreement with the reported presence of N-H bonds in metalorganic vapor phase epitaxy-grown ZnSe films.³ By intentionally injecting H_2 into the chamber during growth, the incorporation of H in MBE-grown ZnSe:N epilayers was also investigated. (In MBE growth, elemental Zn and Se are the constituent species.) Figure 4 shows the SIMS profile of a MBE-grown

³ J.A. Wolk, J.W. Ager, K.J. Duxstand, E.E. Haller, M.R. Taskar, D.R. Dorman, and D.J. Olego, "Local Vibrational Mode Spectroscopy of Nitrogen-Hydrogen Complex in ZnSe," *Appl. Phys. Lett.* 63: 2756-2758 (1993); A. Kamata, H. Mitsuhashi, and H. Fujita, "Origin of the Low Doping Efficiency of Nitrogen Acceptors in ZnSe Grown by Metalorganic Chemical Vapor Deposition," *Appl. Phys. Lett.* 63: 3353-3354 (1993).

ZnSe:N structure incorporating an intentionally hydrogenated layer. The hydrogenated ZnSe:N layer (obtained by the injection of 3 sccm of H_2 through the H_2Se cracker) showed that the [H] was at an elevated concentration although slightly below the [N] level. The unhydrogenated MBE layer, that was grown under identical nitrogen doping conditions, showed that the [N] was at the same concentration but that the [H] was near the background level. The undoped ZnSe layer provided a reference for the background concentration of both nitrogen and hydrogen. Therefore, the presence of H_2 in the growth environment, either intentionally injected or derived from the thermal decomposition of H_2Se , results in an unambiguous dopant enhanced hydrogenation when nitrogen is used as a dopant. In addition, the diffusion of hydrogen in ZnSe:N is small as indicated by the relatively sharp transition in the [H] from the hydrogenated layer to the unhydrogenated layer in the conventionally-grown MBE layer. Based on the observation that the injection of H_2 during MBE, at flows in excess of those typically observed during GSMBE, resulted only in partial hydrogenation, sub-hydride species of

H_2Se that are present due to the incomplete cracking of H_2Se , play a major role in the observed passivation of the nitrogen acceptors. *Ex-situ* post-growth methods of removing the hydrogen, such as rapid thermal anneals at $500^\circ C$ and long term anneals at $600^\circ C$ for one hour, have been unsuccessful in creating conductive p-type ZnSe films that were grown by GSMBE.

In summary, significant hydrogenation in ZnSe:N grown by GSMBE has been observed. Unlike ZnSe:Cl layers grown by GSMBE, where hydrogen was found to be near the background level and was independent of the [Cl], the [H] was found to follow closely the profile of the [N] in ZnSe:N samples. When H_2 was intentionally introduced during the conventional MBE growth of ZnSe:N, enhanced hydrogen incorporation was observed. These results suggest that a significant source of the incorporated hydrogen in these ZnSe:N films may be the presence of a large amount of ambient H_2 in the growth environment, whether it is intentionally injected or present as a by-product of the H_2Se decomposition reaction.

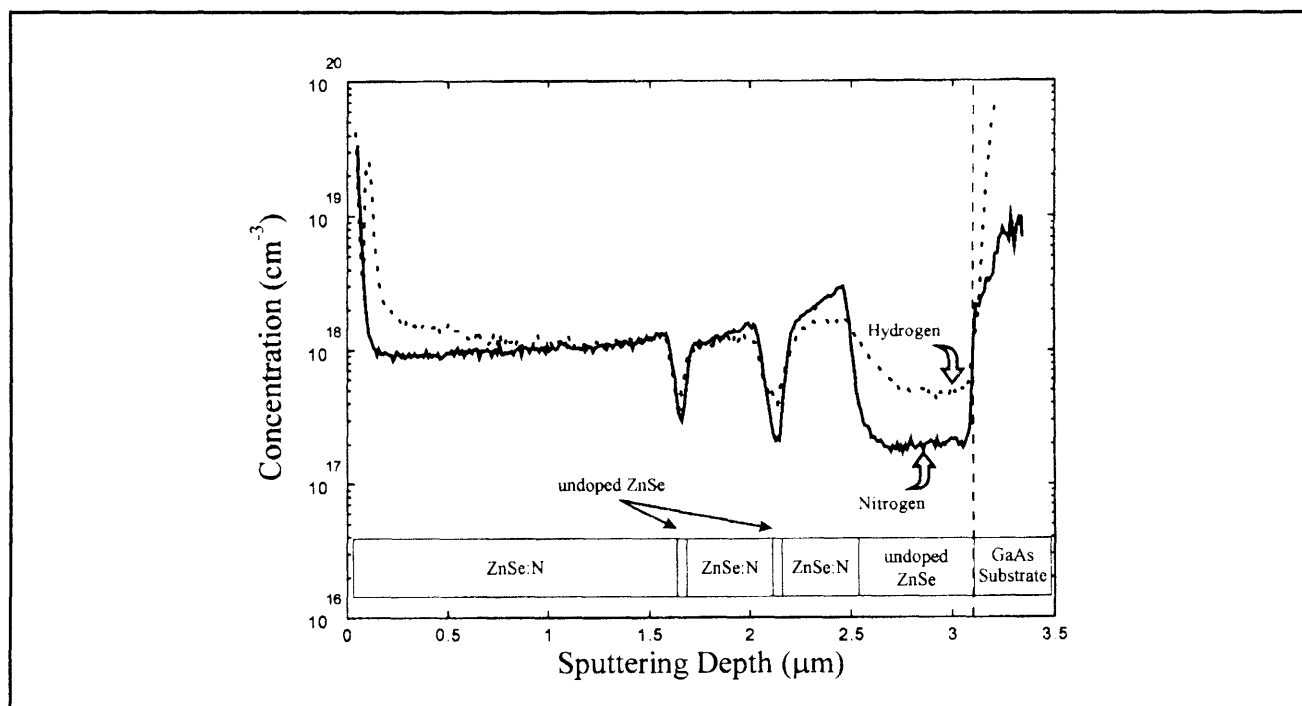


Figure 3. SIMS profile of a ZnSe:N structure grown by GSMBE having an initial undoped layer near the ZnSe/GaAs interface, followed by two thin undoped regions in an otherwise uniformly nitrogen-doped film as schematically indicated in the figure. The sudden rise in the [H] and [N] at the ZnSe/GaAs interface are artifacts of the data normalization process.

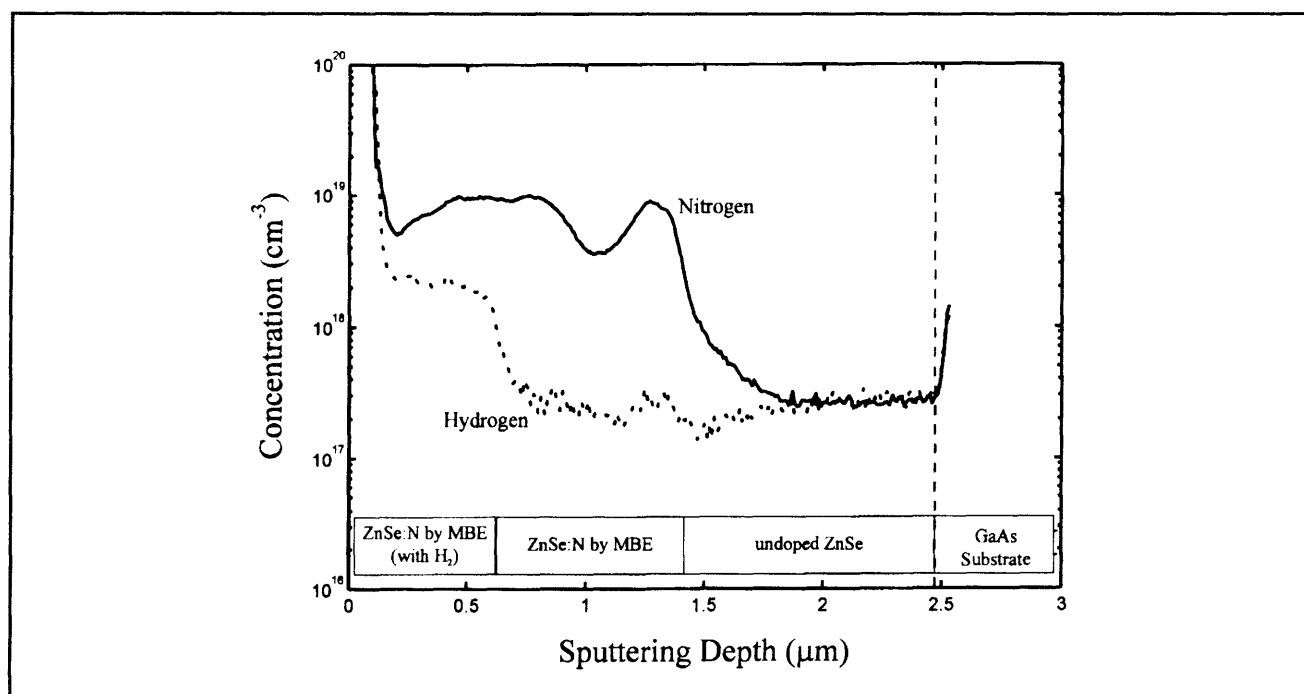


Figure 4. SIMS profile of a ZnSe:N structure (as indicated schematically in the figure) grown by MBE both with and without intentional injection of hydrogen through the H_2Se cracker held at 300°C . The sudden rise in the [H] and [N] at the ZnSe/GaAs interface are artifacts of the data normalization process.

3.2.1 Publications

Coronado, C.A., E. Ho, P.A. Fisher, J.L. House, K. Lu, G.S. Petrich, and L.A. Kolodziejski. "Gas Source Molecular Beam Epitaxy of ZnSe and ZnSe:N." *J. Electron. Mater.* 23: 269-273 (1994).

Fisher, P.A., E. Ho, J.L. House, G.S. Petrich, L.A. Kolodziejski, M.S. Brandt, and N.M. Johnson. "N- and P- Type doping of ZnSe using Gas Source Molecular Beam Epitaxy." *Mat. Res. Soc. Symp. Proc.* 340: 451-456 (1994).

Fisher, P.A., E. Ho, J.L. House, G.S. Petrich, L.A. Kolodziejski, J. Walker, and N.M. Johnson. "P- and N-type Doping of ZnSe: Effects of Hydrogen Incorporation." 8th International Conference on Molecular Beam Epitaxy, Osaka, Japan, August 29-September 2, 1994. *J. Cryst. Growth.* Forthcoming.

Ho, E., P.A. Fisher, J.L. House, G.S. Petrich, L.A. Kolodziejski, J. Walker, and N.M. Johnson. "Hydrogen Passivation in Nitrogen- and Chlorine-Doped ZnSe Films Grown by Gas Source Molecular Beam Epitaxy." *Appl. Phys. Lett.* Forthcoming.

3.3 Novel Epitaxial III-V Buffer Layers for Wide Bandgap II-VI Visible Sources

Sponsors

Advanced Research Projects Agency
Subcontract 284-25041

National Center for Integrated Photonic Technology
Contract 542-381

Grant subcontract 652-693

National Science Foundation

Grant DMR 92-02957

Project Staff

Professor Leslie A. Kolodziejski, Dr. Gale S. Petrich, Philip A. Fisher, Easen Ho, Jody L. House, Kan Lu

A number of important advantages are offered by the use of novel (In,Ga,Al)P epitaxial buffer layers for the subsequent growth of ZnSe-based optical devices. The optimum substrate is bulk ZnSe material; however, ZnSe bulk substrates are very expensive, have a small useable area, and the surface preparation techniques necessary for epitaxy are not well understood. In the past, therefore, the primary substrate employed for ZnSe-based optical devices was GaAs, possessing a small 0.27 percent lattice constant mismatch. As seen in figure 1, the use of the (In,Ga,Al)P quaternary alloy, as an epitaxial buffer layer for

ZnSe growth, provides the opportunity to vary the in-plane surface lattice constant (to match that of ZnSe) and also enables the variation of the energy bandgap of the III-V alloy buffer layer to facilitate the transport of carriers from the substrate into the active region of the II-VI overlayer. The valence-band offset between p-type GaAs and p-type ZnSe is approximately 1 eV. By the insertion of an (In,Al)P buffer layer between the GaAs and the ZnSe, the valence-band discontinuity is expected to be reduced to 0.34 eV, as opposed to 0.67 eV for (In,Ga)P. Appropriate doping and formation of the II-VI/III-V heterovalent interface may further reduce the barrier for hole injection. In addition to the aforementioned advantages, an important current research topic⁴ addresses the formation and propagation of extended defects in ZnSe-based optical emitters which eventually limit device lifetime. The ZnSe/GaAs heterointerface is believed to be the site for the nucleation of stacking faults, which then provide sources of dark line defects.⁵ The use of novel (In,Ga,Al)P buffer layers will offer an alternative interface surface chemistry for exploration, and thus may shed more insight into the problems involving the II-VI/III-V heterovalent interface.

The investigation into the growth of ZnSe on epitaxial (In,Al,Ga)P buffer layers represents a unique contribution to the area of II-VI-based semiconductors by our group at MIT. Our interconnected II-VI and III-V gas source molecular beam epitaxy reactors enable the investigation of the nucleation of ZnSe on epitaxial layers consisting of a multitude of III-V alloys. In the III-V reactor, the various (In,Al,Ga)P buffer layers are grown at 470°C (typically on an epitaxial 0.5 μm thick GaAs buffer layer) where the substrate temperature is calibrated using the melting point of InSb (525°C). Elemental In, Ga, Al and cracked phosphine (thermally decomposed at 900°C) are used as the constituent species. During growth, the (In,Ga,Al)P exhibits a (2x1) surface reconstruction as observed by reflection high energy electron diffraction. The (In,Ga,Al)P film thicknesses range from 0.5-4 μm , and the precise alloy composition and the amount of lattice relaxation are determined from (400) and (511) x-ray diffraction rocking curves. Following growth, the (In,Ga,Al)P films are *in situ* transferred

to the II-VI reactor and the ZnSe growth proceeds in the manner described in the previous section. A variety of characterization techniques are used to analyze the II-VI/III-V heterostructures, and include high resolution double crystal x-ray diffraction, low temperature photoluminescence, optical Nomarski microscopy, and transmission electron microscopy (TEM).

Two parallel paths of investigation have been pursued to address (1) the use of (In,Ga)P buffer layers designed to lattice-match to ZnSe, and (2) the use of (In,Ga,Al)P layers to facilitate transport of carriers from the p-type GaAs into p-type ZnSe. By varying the In mole fraction of (In,Ga)P from 50 percent to 56 percent and by increasing the buffer layer thickness from one to four microns, the (In,Ga)P is found to possess an in-plane surface lattice constant near to that of ZnSe. To release the build-up of strain energy due to the lattice constant mismatch with GaAs, edge-type misfit dislocations are found located at the (In,Ga)P/GaAs interface as evidenced by cross-sectional TEM. These dislocations propagate parallel to the interface and do not appear to propagate into the overlayer of ZnSe. However, the III-V buffer layer is not fully relaxed, and a small degree of lattice-mismatch still resides at the ZnSe/(In,Ga)P interface as evidenced by x-ray diffraction and photoluminescence measurements of the ZnSe.

The study of hole injection from the III-V quaternary buffer layer into the p-type ZnSe layer has thus far consisted primarily of an investigation into the heteroepitaxy of ZnSe on various III-V alloys. A variety of III-V surfaces have been grown consisting of (In,Ga)P, (In,Ga,Al)P, and (In,Al)P which are all pseudomorphic to the GaAs (and hence lattice-mismatched to the ZnSe). The nucleation of ZnSe on each epitaxial surface is observed to proceed in a layer-by-layer fashion due to the observation of reflection high energy electron diffraction intensity oscillations. Photoluminescence measurements of the 1200 Å pseudomorphic ZnSe layers on the various III-V surfaces show spectra exhibiting dominant free exciton transitions and the absence of deep level defect-related luminescence. In addition, all of the ZnSe films with (In,Ga,Al)P or GaAs

⁴ M.A. Haase, P.F. Boude, M.S. Hagedorn, J. Qiu, J.M. DePuydt, H. Cheng, S. Guha, G.E. Hoffer, and B.J. Wu, "Low Threshold Buried Ridge II-VI Laser Diodes," *Appl. Phys. Lett.* 63: 2315-2317 (1993); S. Guha, J.M. DePuydt, J. Qiu, G.E. Hoffer, M.A. Haase, B.J. Wu, and H. Cheng, "Role of Stacking Faults as Misfit Dislocation Sources and Nonradiative Recombination Centers in II-VI Heterostructures and Devices," *Appl. Phys. Lett.* 63: 3023-3025 (1993); S. Guha, J.M. DePuydt, M.A. Haase, J. Qiu, and H. Cheng, "Degradation of II-VI Based Blue-green Light Emitters," *Appl. Phys. Lett.* 63: 3107-3109 (1993).

⁵ D.C. Grillo, Y. Fan, M.D. Ringle, L. He, J. Han, R.L. Gunshor, A. Salokatve, H. Jeon, M. Hovinen, and A.V. Nurmikko, "MBE Growth and Characterization of II-VI Blue/Green Laser Diodes Having CW Operation at Room Temperature," *Mat. Res. Soc. Symp. Proc.* 340: 431-436 (1994).

buffer layers were featureless as observed by optical Nomarski microscopy.

3.3.1 Publications

Lu, K., P.A. Fisher, E. Ho, J.L. House, G.S. Petrich, L.A. Kolodziejski, G.C. Hua, and N. Otsuka. "Gas Source Molecular Beam Epitaxy Growth of ZnSe on (In,Ga)P." *Mat. Res. Soc. Symp. Proc.* 340: 497-502 (1994).

Lu, K., P.A. Fisher, J.L. House, E. Ho, C.A. Coronado, G.S. Petrich, and L.A. Kolodziejski. "Gas Source Molecular Beam Epitaxy Growth of ZnSe on Novel Buffer Layers." *J. Vac. Sci. Technol. B* 12(2): 1153-1155 (1994).

Lu, K., J.L. House, P.A. Fisher, C.A. Coronado, E. Ho, G.S. Petrich, and L.A. Kolodziejski. "(In,Ga)P Buffer Layers for ZnSe-Based Visible Emitters." *J. Cryst. Growth* 138: 1-7 (1994).

3.4 Heterovalent Interfaces Composed of II-VI/III-V Semiconductors

Sponsors

Joint Services Electronics Program
Contract DAAL03-92-C-0001
Grant DAAH04-95-1-0038
National Science Foundation
Grant DMR 92-02957
Grant DMR 90-22933

Project Staff

Professor Leslie A. Kolodziejski, Dr. Gale S. Petrich, Jody L. House

Traditionally, II-VI and III-V compound semiconductors have been treated as separate material systems, each having its own special applications. For example, GaAs has been extensively used in electronic and optical devices that exploit its high room temperature mobility and direct infrared bandgap. In contrast, ZnSe is currently the research focus for blue/blue-green light emitters that are made possible by its large room temperature bandgap of 2.7 eV. However, by jointly employing the properties of these two material families, it should be possible to create a new class of II-VI/III-V heterojunction devices that have unusual

optical and electronic properties due to differences in the energy bandgap, dielectric constants, refractive indices, etc. The energy bandgaps of the II-VI semiconductor cover the visible spectrum and are significantly wider than those of typical III-V compounds (see figure 1). It is also important to note that for every technologically important III-V semiconductor, such as GaAs or InP, there exists a perfectly lattice-matched II-VI ternary counterpart that, when layered together, can provide "defect-free" coherent II-VI/III-V heterointerfaces. (In addition, the thermal expansion coefficients of the II-VI and III-V compounds are, in many cases, quite similar.) In contrast to the similarities of the II-VI and III-V materials, there are large differences in their optical constants. The II-VI compounds typically have a smaller dielectric constant and a lower refractive index than its lattice-matched III-V counterpart. Combining the material properties of the II-VI and III-V compound semiconductors offers the device designer greater flexibility in specifying barrier layers, insulating layers, and waveguiding or optical confinement layers, while maintaining structural compatibility.

In collaboration with Professor E.P. Ippen, the nonlinear optical properties of II-VI/III-V quantum well structures, composed initially of ZnSe/GaAs multilayers, are under investigation. Due to the large differences in the dielectric constants (ZnSe: 8.1, GaAs: 12.0), the layered structures are referred to as dielectric quantum wells. Kumagai and Takagahara⁶ have theorized that for these dielectric quantum well structures an increase in the exciton reduced mass and thus, an enhanced excitonic binding energy, an enhanced oscillator strength, and an enhanced nonlinear optical response is anticipated. Not only can the optical properties of the dielectric quantum well be enhanced, but other material properties will be affected, such as the mobility of the carriers, the RC time constant, and the Frohlich interaction.

The initial structure under investigation is a ZnSe/GaAs/ZnSe single quantum well. The substrates which have been employed include GaAs and ZnSe bulk material, and (In,Ga)P epilayers on GaAs to facilitate appropriate confinement of carriers and to affect the lattice constant mismatch. Again, the interconnected II-VI and III-V GSMBE reactors are crucial for the fabrication of these sophisticated II-VI/III-V heterostructures. The growth of ZnSe on GaAs is well understood; however, the formation of the inverted interface,

⁶ M. Kumagai and T. Takagahara, "Excitonic and Nonlinear-Optical Properties of Dielectric Quantum-Well Structures," *Phys. Rev. B* 40: 12359-12381 (1989).

i.e., GaAs onto ZnSe, has not been previously investigated. Therefore, the initial investigative path consists of the growth of a III-V epilayer of GaAs onto a II-VI epitaxial ZnSe surface. In this case, the II-VI surface has been fabricated in the II-VI reactor and transferred via the transfer chamber into the III-V reactor. In order to avoid interdiffusion of the Zn and Se into the GaAs quantum well, the GaAs is grown at a substrate temperature of 350°C. The growth parameters of the III-V/II-VI heterostructures have been optimized to form abrupt heterointerfaces and to result in the two-dimensional growth of GaAs. The two-dimensional growth of GaAs on ZnSe was successfully achieved by carefully engineering the initial stages of nucleation. Monolayer-controlled GSMBE was employed to reduce the islanding of highly mobile Ga atoms on the ZnSe surface and was only performed during the formation of the interface to enable the careful engineering of the stoichiometry. The Group V-to-Group III flux ratio is carefully maintained at 12-to-1 during the initial nucleation. Following the growth of six monolayers, reflection high energy electron diffraction patterns suggest a smooth GaAs surface and a c(4x4) reconstructed surface.

The growth conditions of the optimized III-V/II-VI heterostructure have been used as the foundation for the growth of ZnSe/GaAs/ZnSe single quantum well (SQW) structures. As previously mentioned, the SQW structure has been grown on both GaAs and ZnSe substrates. (400) x-ray diffraction rocking curves have been used to examine the amount of strain in the quantum well. Figure 5 shows a (400) rocking curve of a 8 nm GaAs quantum well with 50 nm ZnSe barriers. When using either aforementioned substrate, the heterointerfaces are nucleated using the growth conditions which minimize the formation of Ga-Se bonds and thus leads to the most abrupt heterointerface.

The optical properties of the ZnSe/GaAs/ZnSe quantum well will be affected by the presence of the II-VI/III-V heterovalent interface, but is also affected by the growth of the GaAs quantum well at the unusually low temperature of 350°C (the usual growth temperature is 580°C). To enable separate assessment of the effect of the heterovalent interfaces from the effect of the low temperature growth of GaAs, a series of GaAs quantum wells have been fabricated with (In,Ga)P barrier layers. By varying the As-to-Ga flux ratio for growth of GaAs at 350°C, and by varying the quantum well width and growth temperature simultaneously, we have measured photoluminescence originating from a 15 Å GaAs single quantum well grown at 350°C (with (In,Ga)P barrier layers). By inserting this GaAs material between barrier layers of ZnSe and by

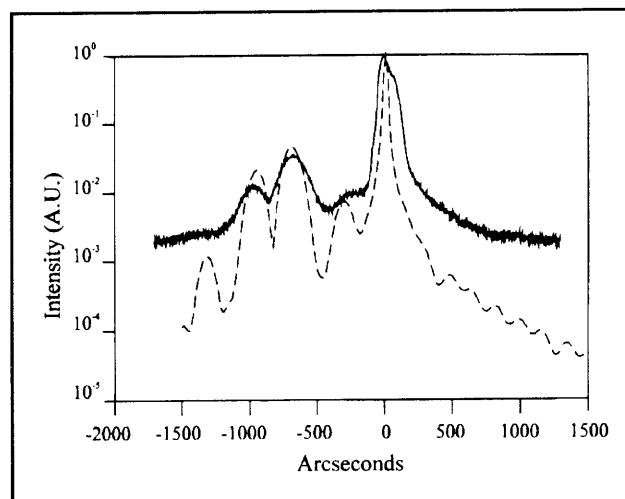


Figure 5. High resolution double crystal x-ray diffraction (400) rocking curve of a 8 nm single GaAs quantum well with ZnSe barriers. The dotted line corresponds to simulation results and the solid line corresponds to the experimental results.

varying the quantum well dimension, the affect of the heterovalent interface is isolated and assessed. Finally, upon the successful fabrication of single quantum well structures consisting of ZnSe/GaAs/ZnSe, the fabrication of superlattice structures will be attempted in a single reactor with gaseous sources for all of the constituent species. The II-VI reactor has been specially equipped to consider the growth of these II-VI/III-V quantum wells.

3.5 (In,Ga)(As,P)/InP Semiconductor Waveguide Design for Synchronously Side-Coupled Bragg Resonators

Sponsors

MIT Lincoln Laboratory
Contract BX-5411
National Center for Integrated Photonic Technology
Contract 542-383
Grant subcontract 652-693

Project Staff

Professor Hermann A. Haus, Professor Leslie A. Kolodziejki, Professor Henry I. Smith, Dr. Gale S. Petrich, Jay N. Damask, Elisabeth A. Marley

In collaboration with Professors Hermann A. Haus and Henry I. Smith, this project involves the fabrication of a channel dropping filter based on the (In,Ga)(As,P) materials system and designed to operate at the optimum wavelength of 1.55 μm for optical communication applications. The theory and

design component of the project resides with Professor Haus, while the fabrication of the layered structure and the formation of the appropriate gratings is performed in the groups of Professors Kolodziejcki and Smith, respectively. The channel dropping filter represents a key optical component for wavelength division de-multiplexing applications. The unique attribute of the channel dropping filter is the ability to selectively "drop" a desired channel, or frequency, from the main waveguide or bus, while sending the other channels undistorted to their final destination. A significant effort is underway to simulate an InP-based channel dropping filter to provide device design constraints on the final fabricated structure.

The channel-dropping filter (figure 6) is constructed by weakly side-coupling two high-Q quarter-wave shifted distributed-Bragg-reflector (QWS-DBR) resonators to a rib waveguide. The resonators are created by etching gratings, each with an appropriately placed quarter-wave shift, on top of the two outer rib waveguides. The period of the grating, ~ 240 nm for the InP material system, is chosen to be the Bragg period of the filter center wavelength. The length of the gratings (e.g., 250-500 μm) are dictated by the required Q of each resonator and the depth of the grating corrugations. The spectral responses at the signal port (top left waveguide) and transmission port (top right waveguide) are shown in figure 6 for a filter designed to maximally

select the on-resonance signal from the center waveguide.

The spectral responses shown in figure 6 were calculated assuming that the phase velocities along the grating and blank waveguides are identical. However, this is generally not the case. The patterning of a grating corrugation on top of the grating waveguide necessarily reduces the effective index of the mode. When a grating waveguide is coupled to a guide with identical dimensions but with no grating, the phase velocities between the two guides are different. The fundamental unit of phase mismatch, ϕ_s , is the phase difference that is accrued over one decay length of the optical mode along the grating length. Figure 7 shows two plots of the same receiver spectrum as in figure 6 but where the phase velocities are mismatched. The spectra is clearly distorted.

Optimal design rules have been determined in order to derive the vertical and lateral dimensions of a coupled waveguide pair such that after the grating is etched, the two guides are synchronous. Figure 8 shows the mode profiles of a blank (rib) and resonator (grating) waveguide where the waveguide widths are 1.0 μm and 2.0 μm , respectively. The differences in effective indices, Δn_{eff} , for these two guides is $\Delta n_{\text{eff}} \approx 0.2 \times 10^{-3}$ or $\phi_s \approx \pi/100$. Such close phase matching would result in acceptable filter performance.

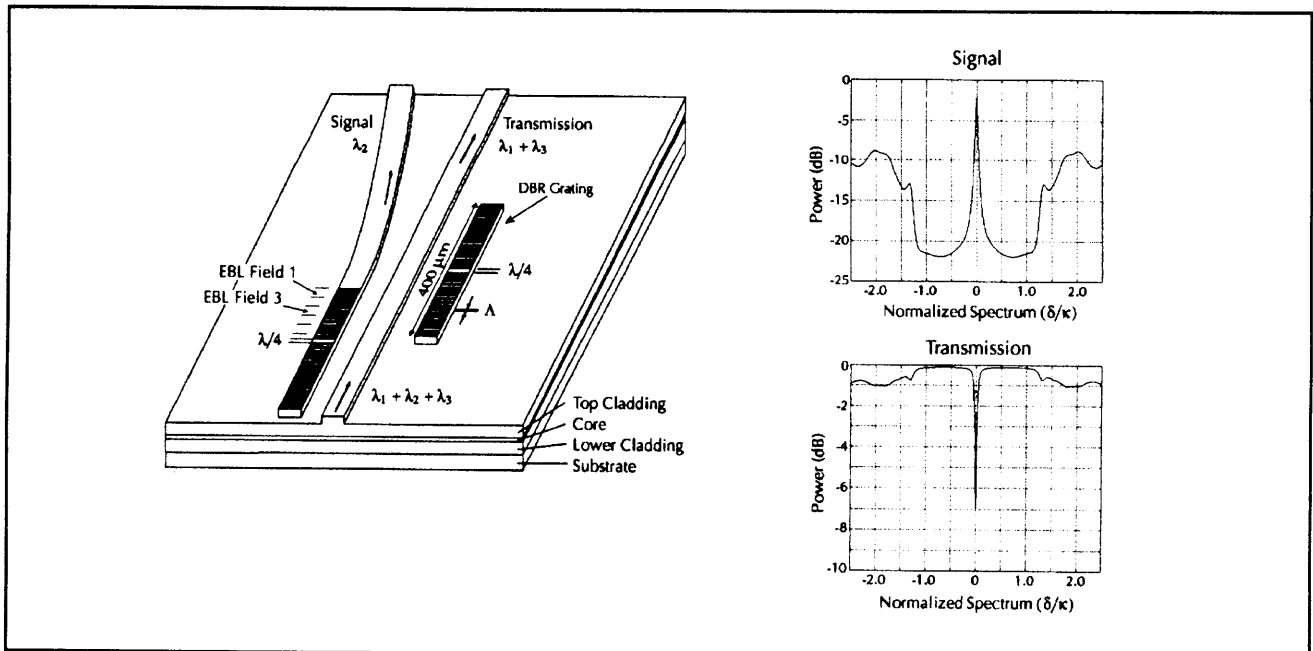


Figure 6. An illustration of the integrated-resonant channel-dropping filter. Two Bragg-grating resonators are weakly side-coupled to the center optical bus in order to remove only the on-resonant signal from the bus. The calculated receiver (signal) and transmission impulse responses show the channel selectivity.

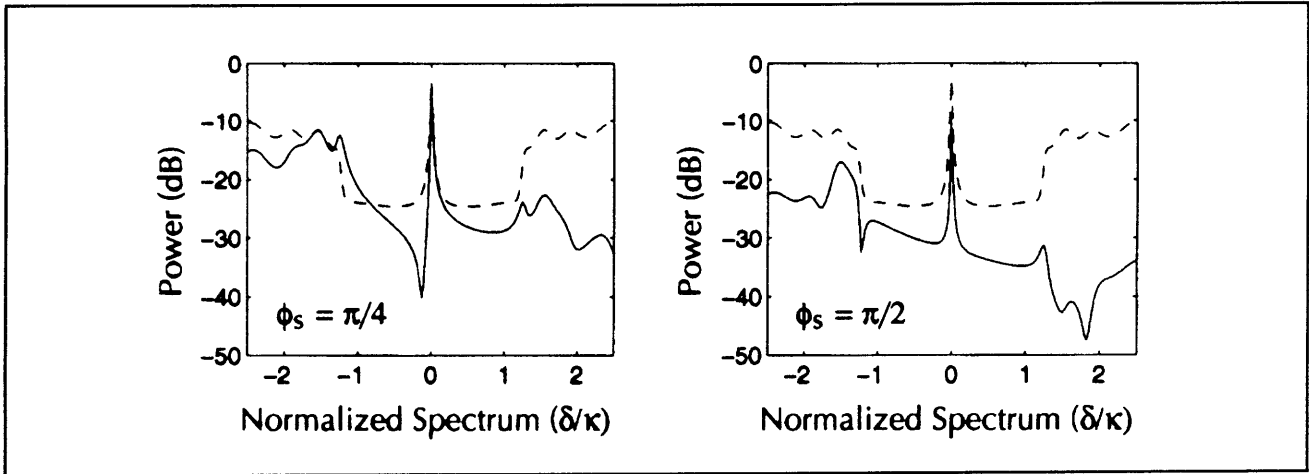


Figure 7. The phase mismatch between two asynchronous waveguides results in the distortion of the optical response of the channel-dropping filter. The phase slip is defined as $\phi_s = 2\pi \Delta n_{\text{eff}}/\kappa \lambda_0$ where κ is the grating strength.

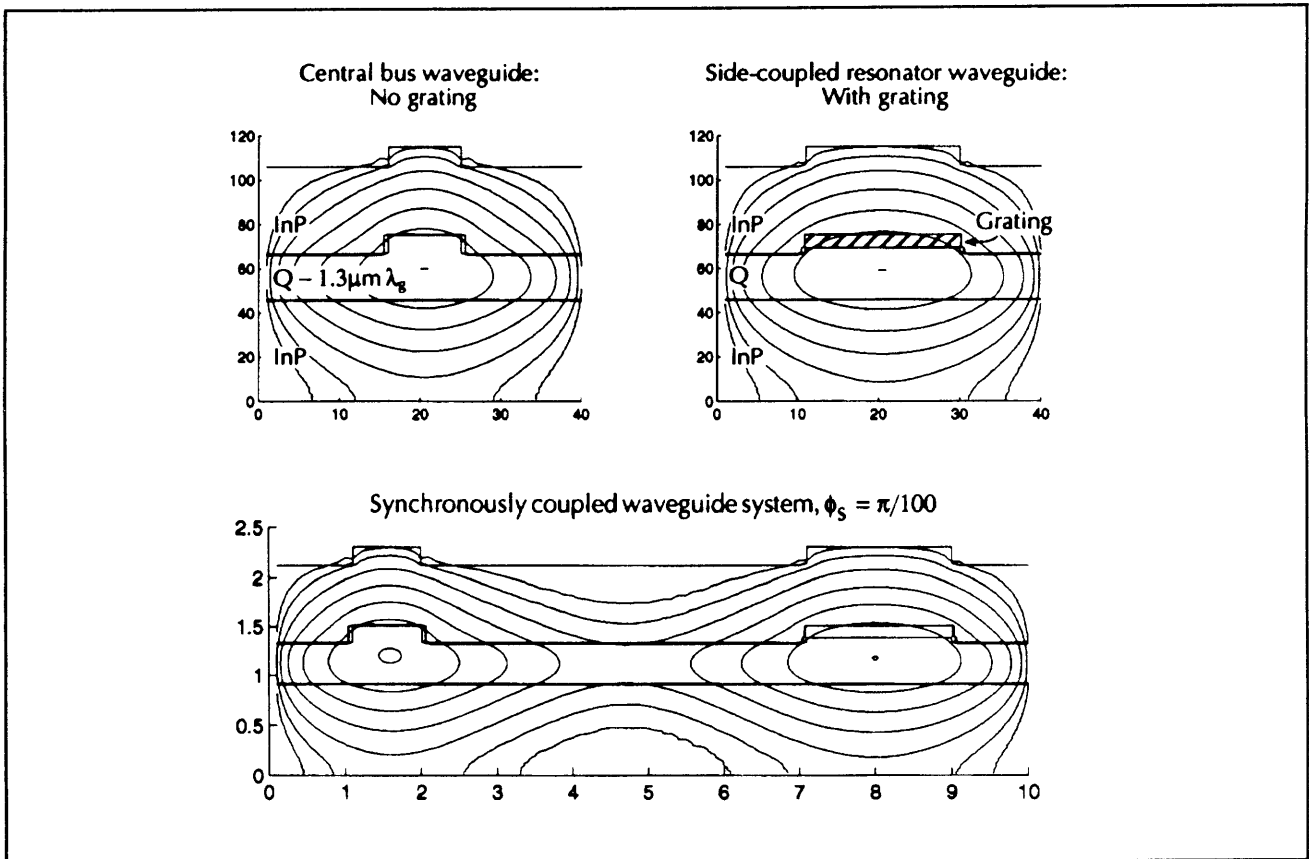


Figure 8. The top two figures show the calculated field profiles of the bus (rib) and resonator (grating) waveguides for an optimally-designed synchronous pair of waveguides. The mode overlap is as low as 99 percent while the effective index difference is only $\Delta n_{\text{eff}} \approx 0.2 \times 10^{-3}$. The grating strength is estimated to be $\sim 260 \text{ cm}^{-1}$, which would result in a $\sim 6 \text{ nm}$ stop band. The bottom shows the calculated field profiles of the coupled system. The inter-most circular field contours under the two waveguides show the difference in optical confinement that was built into the system. In the figure, Q refers to an (In,Ga)(As,P) quaternary alloy.

To fabricate the above design, the core (In,Ga)(As,P) material must be segmented into three layers with InP etch stops positioned at the

correct layer dimension. Tolerance calculations show that the core refractive index, which is related to the (In,Ga)(As,P) composition, must be controlled

to better than ± 0.6 percent to maintain an effective-index mismatch to within $|\Delta n_{\text{eff}}| \leq 0.001$. Furthermore, when the three-level segmented core is grown, the core thicknesses will only be estimated from a time/growth-rate product. If the actual growth rate changes from wafer to wafer, but the target times are held fixed, then the three thicknesses of the segmented core will scale. The tolerance on run-to-run growth-rate variation, as long as the growth rate remains constant during growth, is as large as ± 20 percent while Δn_{eff} remains within $|\Delta n_{\text{eff}}| \leq 0.001$.

Using the III-V-dedicated GSMBE reactor, the growth of a variety of (In,Ga)(As,P) quaternary layers have been fabricated to understand the affect of the Group V overpressure on the quaternary composition. The Group III flux ratio is more easily maintained by establishing the proper effusion cell temperatures. Appropriate composition is necessary to establish the energy bandgap (and hence refractive index), but also to ensure that the layer remains lattice-matched to the InP substrate.

3.5.1 Publications

Damask, J.N., J. Ferrera, V.V. Wong, H.I. Smith, and H.A. Haus. "Limitations and Solutions for the Use of Integrated QWS-DBR Resonators in WDM Applications." *Proceedings of the SPIE International Symposium on Integrated Optical Conference on Nanofabrication Technologies and Device Integration*, Lindau, Germany, April 1994. 137: 2213, (1994).

Wong, V.V., J. Ferrera, J.N. Damask, J. Carter, E.E. Moon, H.A. Haus, H.I. Smith, and S. Rishton. "Spatial-Phase Locked E-beam Lithography and X-ray Lithography for the Fabrication of First-Order Gratings on Rib Waveguides." *J. Vac. Sci. Technol. B* 12(6): 3741-3745 (1994).

3.6 Phosphide-Based Optical Emitters for Monolithic Integration with GaAs MESFETs

Sponsor

National Center for Integrated Photonic Technology
Contract 542-381
Grant subcontract 652-693

Project Staff

Professor Clifton G. Fonstad, Jr., Professor Leslie A. Kolodziejcki, Dr. Gale S. Petrich, Joseph F. Ahadian, Krishna V. Shenoy

A technology thrust aimed at developing a VLSI optoelectronic integrated circuit (OEIC) platform has, under the direction of Professor Fonstad, produced an "Epi-on-Electronics" (E-o-E) monolithic integration method in which optical devices are grown in foundry opened "epitaxy windows" on completed, fully-processed refractory metal GaAs VLSI MESFET circuits.⁷ These VLSI chips, commercially manufactured by Vitesse Semiconductor Co. and available through MOSIS, have been found to withstand extended temperature cycles of up to approximately 500°C without significant degradation of the electronic devices, and thus suggest the possibility of subsequent growth of optical devices using molecular beam epitaxy (MBE). A difficulty, however, is that substrate temperatures less than 500°C are not optimal for the conventional MBE-growth of AlGaAs-containing LEDs and lasers; these devices exhibit compromised performance. High performance lasers, utilizing InGaP (In_{0.49}Ga_{0.51}P is lattice matched to GaAs) as the wide bandgap material, have been realized by a number of groups.⁸ Since phosphorus-containing alloys are nominally grown by gas source MBE below 500°C, the integration of high quality LEDs and lasers based on this material system is the objective of the current project utilizing our III-V-dedicated GSMBE reactor.

Our current emphasis involves (In,Ga)As quantum wells inserted between cladding layers of GaAs, as well as (In,Ga)P. Although GaAs is typically grown at 580°C, for our study the thin layers of GaAs (and InGaAs) are grown at 470°C, which is the desired

⁷ A.C. Grot, D. Psaltis, K.V. Shenoy, and C.G. Fonstad Jr., "Integration of LED's and GaAs Circuits by MBE Regrowth," *IEEE Photon. Tech. Lett.* 6: 891-821 (1994); K. Shenoy, C.G. Fonstad Jr., and J.M. Mikkelsen, "High-Temperature Stability of Refractory-Metal VLSI GaAs MESFETs," *IEEE Electron. Dev. Lett.* 15: 106-108 (1994).

⁸ J.M. Kou, Y.K. Chen, M.C. Wu, and M.A. Chin, "InGaAs/GaAs/InGaP Multiple-Quantum-Well Lasers Prepared by Gas-Source Molecular Beam Epitaxy," *Appl. Phys. Lett.* 59: 2781-2783 (1991); G. Zhang, J. Nappi, K. Vanttinen, H. Asonen, and M. Pessa, "Low Threshold Current Strained-Layer InGaAs/GaAs/InGaP Lasers Grown By Gas-Source Molecular Beam Epitaxy," *Appl. Phys. Lett.* 61: 96-98 (1992).

temperature for growth of the (In,Ga)P and (In,Ga)As layers. InGaP/GaAs/InGaAs quantum well separate confinement heterostructure lasers having threshold current densities of 220 A/cm^2 (for pulsed room temperature broad-area devices) have been fabricated (figure 9). Electroluminescence measurements on InGaP/GaAs double heterostructures have shown the efficacy of LEDs based on this structure (figure 10). However, the aforementioned structures have, thus far, been grown on bulk GaAs. Simultaneous growth within the "epitaxy windows" on the VLSI chips resulted in a very rough, highly defective surface morphology, which contrasts to the occurrence of a smooth, nearly featureless morphology on the bulk substrate. It immediately became apparent that the surface of the "epitaxy windows" was not properly prepared for epitaxy. Therefore, two remaining challenges to the integration process are now being addressed. First, the normal MBE practice of briefly elevating the substrate temperature (to around 600°C) to desorb the native GaAs oxide prior to epitaxy must be eliminated since it damages the upper-level metal interconnects. The technique under investigation uses a hydrogen plasma in the II-VI reactor to remove the oxide at a substrate temperature of $\sim 300^\circ\text{C}$. The second challenge is to develop a more robust procedure for preparing the "epitaxy windows" for growth, ensuring more reliable epitaxy results. These innovations will allow the integration of state-of-the-art emitters onto a VLSI optoelectronic integrated circuit.

3.7 Photonic Bandgap Structures

Sponsor

National Science Foundation
DMR 94-00334

Project Staff

Professor John D. Joannopoulos, Professor Leslie A. Kolodziejski, Professor L. Rafael Reif, Dr. Gale S. Petrich, Kuo-Yi Lim, Xiaofeng Tang

A photonic bandgap crystal is a periodic arrangement of dielectric scattering centers within a host dielectric matrix. The effect of the photonic bandgap crystal on the properties of photons is much like the affect of a periodic arrangement of atoms on the behavior of charge carriers. In many ways, the creation of an energy bandgap for carriers in a semiconductor is directly analogous to the creation of a photonic bandgap for photons in a photonic bandgap crystal. The periodic arrangement of the dielectric scattering centers, the discontinuity in dielectric constant between the scatterer and the host matrix, and the length scale associated with the scatterers contribute to determining the size of the photonic bandgap, as well as the frequency or wavelength of the photons affected by the photonic bandgap crystal. In this research project, both one-dimensional and three-dimensional photonic bandgap crystals are under

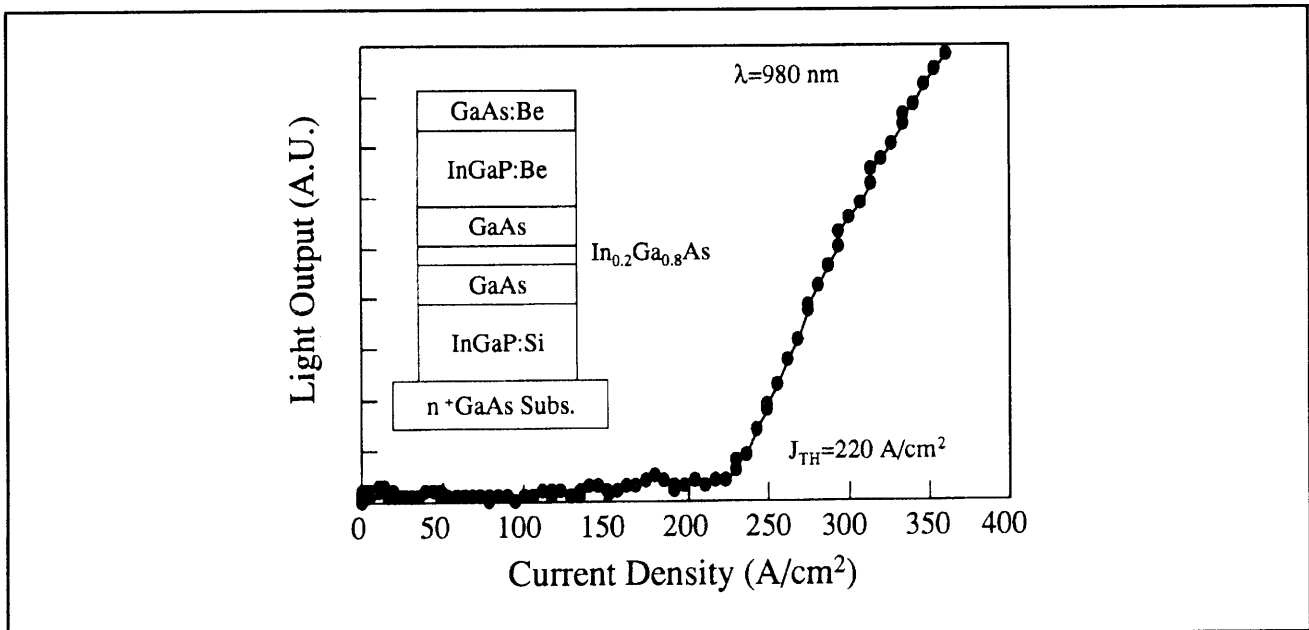


Figure 9. Light output versus current density for a room temperature pulsed broad-area InGaP/GaAs/InGaAs quantum-well separate confinement heterostructure laser. The measured low threshold current density verifies that high quality optical emitters based on this material system, and grown at 470°C , are possible. The inset shows a schematic of the laser structure.

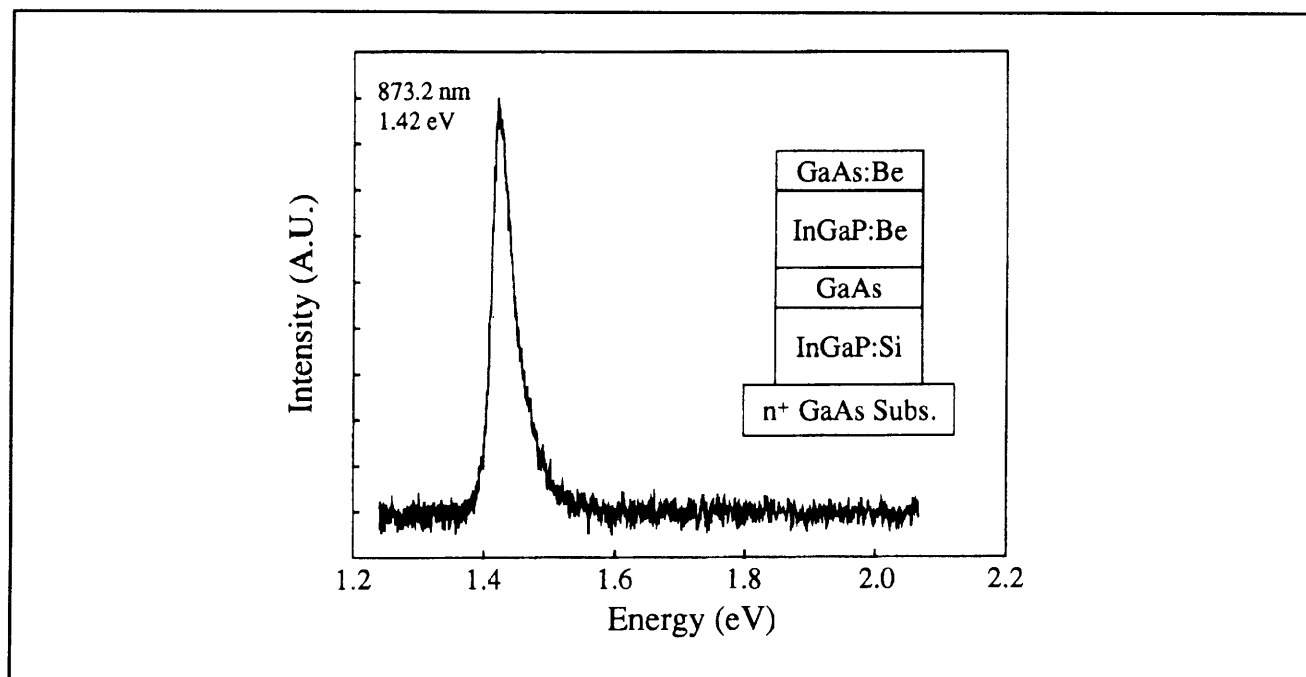


Figure 10. Electroluminescence from a InGaP/GaAs double heterostructure (inset shows a schematic) grown at 470°C. LEDs will be fabricated using this epitaxial structure.

investigation from the point of view of device fabrication, specifically for optical devices affecting 1.55 μm photons. Although the three-dimensional photonic bandgap structure has been simulated theoretically, the device fabrication is still in its infancy. Only the success in the fabrication of the one-dimensional structure will be described here.

A theoretical simulation of a semiconductor air bridge, containing holes that are placed periodically along the length of the bridge, shows that the electromagnetic radiation is confined within the air bridge in all three directions.⁹ Due to the periodicity of the holes (or dielectric scatterers) in the air bridge, the structure exhibits a photonic bandgap as a range of frequencies will not propagate within the bridge. The placement of a "defect", which locally disturbs the periodicity of the holes along the air bridge, creates a microcavity such that there is a high spatial concentration of a single electromagnetic mode. The Q factor of such a state has been calculated to exceed 13000.¹⁰ By adjusting the geometry of the system, the single mode of the microcavity can be placed within the photonic

bandgap of the air bridge and thus leads to the possibility of a semiconductor laser having a very low threshold current. Currently, initial prototypes of the semiconductor air bridges have been fabricated using Si/SiO₂ on Si substrates and GaAs/AlAs on GaAs substrates (figure 11). The thicknesses of each bridge was 0.5 μm . To create a semiconductor air bridge, the holes and the bridge are defined using reactive ion etching, and the material that is under the bridge is removed by selective wet chemical etching. The next generation of the one-dimensional photonic bandgap crystal will incorporate a waveguide leading to the air bridge in order to measure the transmission, and hence photonic bandgap, of the air bridges.

3.7.1 Publication

Villeneuve, P.R., S. Fan, J.D. Joannopoulos, K.Y. Lim, G.S. Petrich, L.A. Kolodziejski, and R. Reif. "Air-Bridge Microcavities." Submitted to *Phys. Rev. Lett.*

⁹ R.D. Meade, A. Devenyi, J.D. Joannopoulos, O.L. Alerhand, D.A. Smith, and K. Kash, "Novel Applications of Photonic Band Gap Materials: Low-loss Bends and High Q Cavities," *Appl. Phys. Lett.* 75: 4753-4755 (1994).

¹⁰ S. Fan, J.N. Winn, A. Devenyi, R.D. Mead, and J.D. Joannopoulos, "Guided and Defect Modes in Periodic Dielectric Waveguides," *J. Opt. Soc. Am. B*, forthcoming.

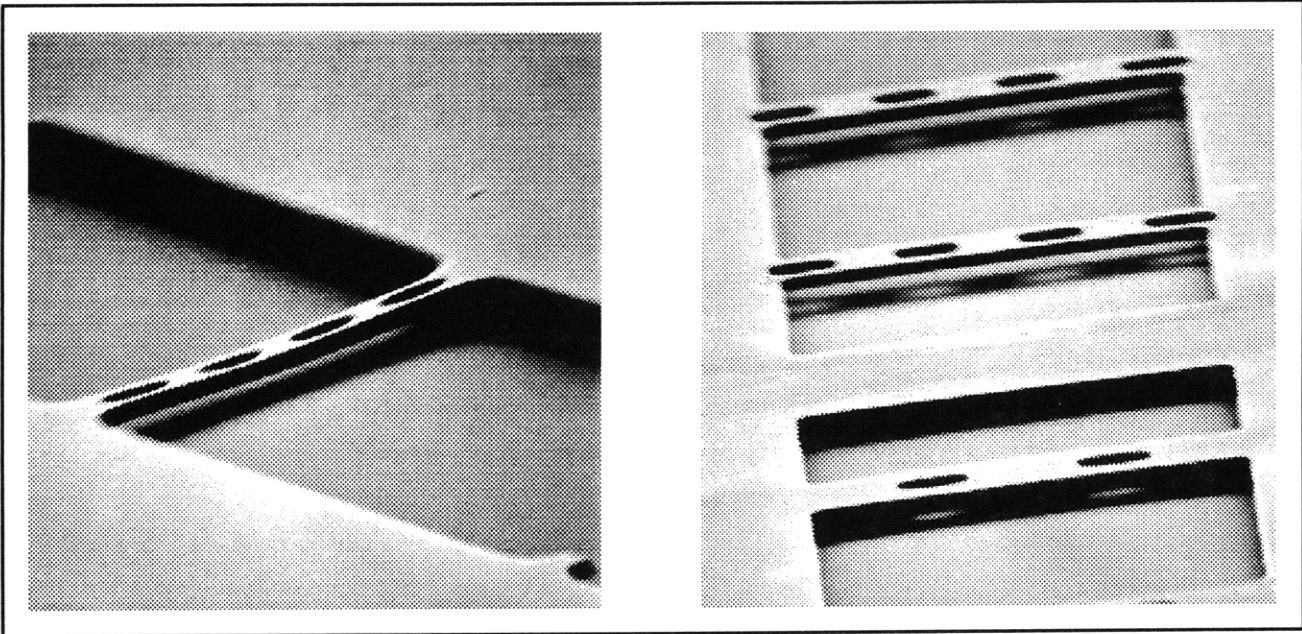


Figure 11. (left) SEM photograph of the Si bridge. The bridge has a length of $10\ \mu\text{m}$ and a width of $4\ \mu\text{m}$. The holes are $2\ \mu\text{m}$ in diameter and are separated by $3\ \mu\text{m}$ from center to center. (right) SEM photograph of GaAs bridges. The bridges are $20\ \mu\text{m}$ in length and range from 3.5 to $5.5\ \mu\text{m}$ in width. The holes are all $2.5\ \mu\text{m}$ in diameter and are separated from center to center by $7.5\ \mu\text{m}$ (foreground) and $5\ \mu\text{m}$ (background).

3.8 Heteroepitaxy of GaAs onto Corrugated Surfaces of Si

Sponsor

Joint Services Electronics Program
Contract DAAL03-92-C-0001
Grant DAAH04-95-1-0038

Project Staff

Professor Leslie A. Kolodziejski, Professor Henry I. Smith, Professor Carl V. Thompson, Dr. Gale S. Petrich, Sean M. Donovan

GaAs-based devices provide unique optoelectronic capabilities which are not available with Si-based devices. However, the processing technology for GaAs is not as mature as for Si VLSI processing technology. A natural step would be to combine the two device systems via monolithic integration, requiring the heteroepitaxial growth of GaAs onto Si substrates. Problems arise however from the 4.1 percent lattice constant mismatch and the large dif-

ference in thermal expansion coefficients occurring between GaAs and Si. Lattice constant and thermal expansion coefficient mismatch lead to the development of unacceptably high dislocation densities in the GaAs overlayer prohibiting the fabrication of optical devices. In earlier work by Professor Henry I. Smith and coworkers,¹¹ the growth of GaAs films on Si substrates, etched with a saw-tooth profile having a periodicity of $200\ \text{nm}$, resulted in a profound reduction of threading dislocations. A study is underway to determine the mechanism responsible for the reduction in dislocation density; this will result in the successful integration of GaAs and Si devices. Gas source molecular beam epitaxy is utilized for GaAs film growth on Si, where the high temperature *in situ* Si substrate cleaning step is avoided. This is essential for the monolithic integration of GaAs and Si devices. The study will also aid in the understanding of polar on non-polar epitaxy using GaAs-on-Si as a test structure. Current work is primarily focusing on establishing the optimal growth conditions for GSMBE of GaAs on Si substrates.

¹¹ K. Ismail, F. Legoues, N.H. Karam, J. Carter, and H.I. Smith, "High-quality GaAs on Sawtooth-Patterned Si Substrates," *Appl. Phys. Lett.* 59: 2418-2420 (1991).

